Nano Research 2016, 9(7): 2088–2096
DOI 10.1007/s12274-016-1099-5
Research Article
ISSN 1998-0124
CN 11-5974/O4

Dual-emissive nanohybrid of carbon dots and gold nanoclusters for sensitive determination of mercuric ions

Yehan Yan[1,2,3], Huan Yu[2,3], Kui Zhang[2], Mingtai Sun[2], Yajiao Zhang[2,3], Xiangke Wang[1], and Suhua Wang[1,2,3] (✉)

[1] *School of Environment and Chemical Engineering, North China Electric Power University, Beijing 102206, China*
[2] *Institute of Intelligent Machines, Chinese Academy of Sciences, Hefei 230031, China*
[3] *Department of Chemistry, University of Science and Technology of China, Hefei 230026, China*

Received: 21 February 2016
Revised: 7 April 2016
Accepted: 9 April 2016

KEYWORDS
Au nanoclusters, carbon nanodots, nanohybrid probe, mercury ion

ABSTRACT

The present work reports a sensitive and selective fluorescent sensor for the detection of mercury ion, Hg(II), by hybridizing carbon nanodots (C-dots) and gold nanoclusters (Au NCs) through intrinsic interactions of the two components. The C-dots serve as the reference signal and the Au NCs as the reporter. This method employs the specific high affinity metallophilic Hg^{2+}–Au^{+} interactions which can greatly quench the red fluorescence of Au NCs, while the blue fluorescence of C-dots is stable against Hg(II), leading to distinct ratiometric fluorescence changes when exposed to Hg(II). A limit of detection of 28 nM for Hg(II) in aqueous solution was estimated. Thus we applied the sensor for the detection of Hg(II) in real water samples including tap water, lake water and mineral water samples with good results. We further demonstrated that a visual chemical sensor could be manufactured by immobilizing the nanohybrid probe on a cellulose acetate circular filter paper. The paper-based sensor immediately showed a distinct fluorescence color evolution from pink to blue after exposure to a drop of the Hg(II) solution.

1 Introduction

Mercury pollution due to human activities has always been an environmental concern because of its highly toxic and widespread emissions. The metallic ions are readily absorbed into human bodies and get accumulated because of their non-biodegradable and bio-accumulative property. This can result in a variety of damages to the human brain, the heart and the kidneys and even permanent damage to the central nervous system and the other organs [1–3]. Currently, the widely used methods for mercuric ion (Hg(II)) analysis include cold-vapor atomic absorption spectrometry [4, 5], X-ray absorption spectroscopy [6–8], inductively coupled plasma-mass and cold-vapor atomic fluorescence spectrometry [9–11]. These

Address correspondence to shwang@iim.ac.cn

conventional lab and instrument-based methods can help little for on-site and rapid mercuric screening from the view point of environment protection and pollution control. Recently, certain chemical sensors based on optical signals have been reported for Hg(II), such as, colorimetric assay using nanoparticles (NP) of Au, Ag and Cu [12–14], electrochemical sensors [15, 16] and fluorescence method based on organic molecules (fluorophores or chromophores) [17, 18] and inorganic nanomaterials (nanoclusters (NC) of Ag or Au) [19–24]. Fluorescence-based analytical methods have been proven to be a promising alternative for the determination of Hg(II) in aqueous solutions because of their unique optical properties, simple synthesis techniques, high intrinsic sensitivities and rapid analyses. However, the optical method has greatly relied on the development of new fluorescent materials, especially the fluorescent nanomaterials.

Carbon nanodots (C-dots) are novel fluorescent nanomaterials which have become popular in recent years because of their particular fluorescent properties, water solubility, high quantum yield, good photostability, lower cytotoxicity and excellent biocompatibility [25–27]. In addition, gold nanoclusters with high fluorescent quantum yield have been reported, which are also attractive because of their ultrafine size, good photostability and low toxicity [28, 29]. These optical properties of C-dots and Au NCs make them advantageous over luminophores such as organic dyes, and semiconductor quantum dots. This is because luminophores are generally prone to photobleaching and semiconductor quantum dots typically contain toxic metal ions such as cadmium. Therefore, it is beneficial to design chemical sensors using the two fluorescent nanomaterials.

In the present work, we have synthesized a sensitive ratiometric fluorescence probe by exploiting the superior optical properties of C-dots and Au NCs, by hybridizing them to form a dual-emissive fluorescent probe for sensitive detection of Hg(II). Such a design for the dual-fluorescence probe was inspired by the following facts: (i) Au NCs are susceptible to reactions with Hg(II) due to the specific and strong d^{10}–d^{10} metallophilic interactions ((Hg^{2+}) $5d^{10}$–$5d^{10}$ (Au^{+})), [21, 30, 31] and (ii) C-dots exhibit excellent chemical inertness to heavy metal ions, which can be used as a reference signal. Thus, the different responses of the blue fluorescent C-dots and the red fluorescent Au NCs of the dual-emission probe to Hg(II) can be used for the visualization of Hg(II) by the distinct fluorescence color change. However, a single fluorescence signal is easily influenced by the experimental conditions such as, temperature, instrumental condition, probe concentration, solvent polarity, etc. Contrary to the single fluorescence measurement, ratiometric fluorescence sensing based on dual-emission involves simultaneous measurement of two fluorescence signals at different wavelengths, which could exclude or correct the above mentioned unfavorable conditions, thus achieving a more precise and sensitive detection [32–35].

The probe reported in the present study shows a limit of detection of 28 nM in aqueous solution, and this method was also successfully applied to detection of Hg(II) in tap water, lake water and mineral water samples. More importantly, a portable paper sensor was developed for visual detection of Hg(II) in aqueous solution made possible by the appearance of a different fluorescence color under a UV lamp, indicating the potential for practical applications such as on-site Hg(II) detection.

2 Experimental

2.1 Chemicals and materials

All chemicals were of analytical grade and used without further purification. L-proline, sodium borohydride ($NaBH_4$), gold chloride solution ($HAuCl_4$), bovine serum albumin (BSA), cobalt chloride hexahydrate ($CoCl_2{\cdot}6H_2O$), zinc chloride ($ZnCl_2$), copper chloride dihydrate ($CuCl_2{\cdot}2H_2O$), ferric chloride hexahydrate ($FeCl_3{\cdot}6H_2O$), cadmium chloride hydrate ($CdCl_2{\cdot}2.5H_2O$), nickel chloride hexahydrate ($NiCl_2{\cdot}6H_2O$), magnesium chloride hexahydrate ($MgCl_2{\cdot}6H_2O$), sodium chloride (NaCl), potassium chloride (KCl), calcium chloride anhydrous ($CaCl_2$), lead nitrate ($Pb(NO_3)_2$) and mercury nitrate ($Hg(NO_3)_2$) were purchased from Sinopharm Chemical Reagent Co. Ltd. All the reagent solutions were prepared by the water purified through a Millipore system with a resistance of 18.2 MΩ·cm.

2.2 Synthesis of water-soluble C-dots

The highly water-soluble and photoluminescent C-dots were prepared by a simple one-pot hydrothermal method with minor modifications [26]. Typically, L-proline (1.15 g/20 mL) aqueous solution was added into a 50 mL autoclave tube and the solution was sealed and treated at 200 ˚C for 4 h. The resulting brown solution was cooled to room temperature naturally and filtered through 0.45 μM Suporfilters to remove the large or agglomerated particles. Then the C-dots solution was purified by dialyzing against pure water using a membrane (M_W = 3.5 kDa) for 6 h and then storing at 4 ˚C for further use.

2.3 Synthesis of BSA-Au nanoclusters

All the glasswares were first washed with aqua regia and then rinsed with ultrapure water, several times before use. Au NCs were synthesized and purified according to the literature [28]. In a typical experiment, $HAuCl_4$ solution (5 mL, 10 mM) was added to the BSA solution (5 mL, 50 mg/mL) under vigorous stirring. After 5 min, NaOH (0.5 mL, 1 M) solution was introduced to the mixture to adjust the pH to 11.0 and then the mixture was kept under stirring for 12 h at 37 ˚C. The solution color changed from pale yellow to dark orange with red emission, indicating the formation of BSA-Au NCs. The BSA-Au NCs sample was stored at 4 ˚C for future use.

2.4 Synthesis of the nanohybrid probe

The nanohybrid system was prepared by the following procedure. First, 10 μL of the as-prepared C-dots solution and 10 μL of the obtained Au NCs solution were thoroughly mixed in 1.98 mL ultrapure water. The mixture was kept under vigorous stirring for surface hybridization through reaction and interaction. Then, the fluorescence spectrum of the ratiometric probe was collected from 380 to 850 nm, and it exhibited two emissions at 450 and 656 nm. The fluorescence stability of the ratiometric probe and its relative fluorescence ratio intensity, I_{656}/I_{450} were also monitored under a single wavelength excitation. In addition, the stability of the nanohybrid was examined by monitoring the ratiometric fluorescence intensity after centrifugation and dialysis. It was found that the fluorescence spectra and fluorescence color of the nanohybrid did not show a significant change after centrifugation and dialysis (Fig. S1, in the Electronic Supplementary Material (ESM)), implying its good physical stability.

2.5 Determination of Hg^{2+} using the nanohybrid probe

To evaluate the sensitivity of the ratiometric probe for the mercuric ion, various concentrations of Hg(II) (0.0, 100, 200, 300, 400 and 500 nM) were added into the nanohybrid solution in a spectrophotometer quartz cuvette. Subsequently, the fluorescence spectra were recorded from 380 to 850 nm after each addition, under excitation at 365 nm, and slit width of 10 nm. To further study the specificity of the sensing system towards detecting Hg(II) over other environmentally relevant metal ions, the fluorescent properties of the nanohybrid probe in the presence of relevant metal ions (including Na(I), K(I), Ca(II), Mg(II), Ba(II), Zn(II), Co(II), Ni(II), Cd(II), Al(III), Fe(III), Pb(II) and Cu(II)) were carefully examined at the same condition. The average data from three independent measurements were obtained.

2.6 Instrumentation

Fluorescence spectra were recorded using a Perkin-Elmer LS-55 luminescence spectrometer. The transmission electron microscopy (TEM) images were recorded using a JEOL 2010 transmission electron microscope. Fourier transform infrared (FT-IR) spectra were acquired from a Thermo Fisher Nicolet iS10 FT-IR spectrometer. The amount of Hg(II) ion in the water samples was analyzed by an atomic absorption spectrometer (TAS-990). Photographs were taken with a Canon 350D digital camera under a 365 nm UV lamp.

3 Results and discussion

3.1 Characterization of the as-prepared Au NCs and C-dots

The properties of the as-prepared Au NCs and C-dots were investigated by fluorescence spectroscopy, TEM, and FT-IR spectra. Figure 1 shows the maximum emission center of Au NCs at 656 nm, and the C-dots

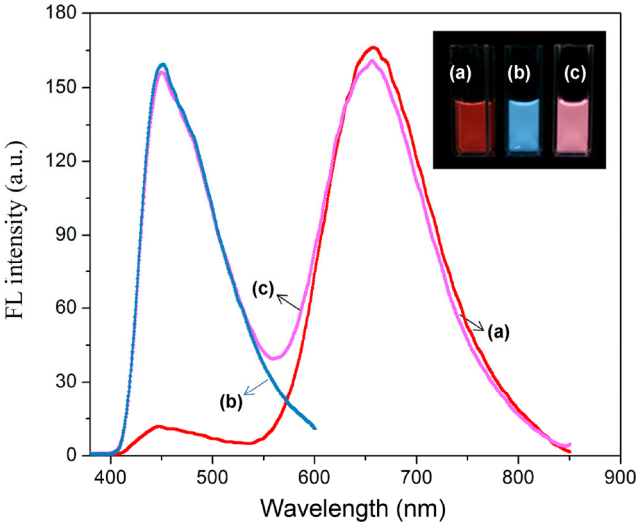

Figure 1 Fluorescence spectra of (a) red emission of BSA-Au NCs, (b) blue emission of C-dots and (c) the nanohybrid system. Inset: the corresponding fluorescence photos taken under a 365 nm UV lamp.

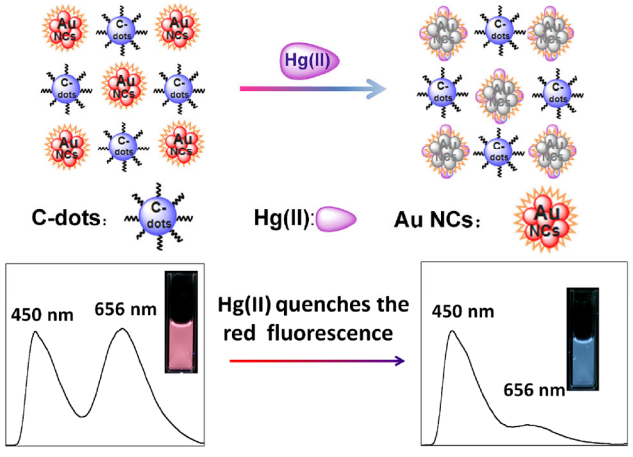

Scheme 1 The scheme of a nanohybrid system for mercury ion detection. The red fluorescence of Au NCs is quenched by Hg(II), while the blue fluorescence of C-dots stay stable to Hg(II), resulting in a color change from pink to blue.

emission band at 450 nm. In the inset of Fig. 1, it can be observed that the solution of fluorescent Au NCs emits intense red fluorescence (Fig. 1(a)) while the solution of C-dots displays blue fluorescence (Fig. 1(b)), under 365 nm UV light. The fluorescence spectra of Au NCs and C-dots were further recorded every 5 min for 1 h under ultraviolet irradiation at 365 nm (Figs. S2 and S3 in the ESM, respectively). Clearly, the fluorescence intensities exhibit no distinct change, implying that both the Au NCs and C-dots exhibit good stability against photobleaching in aqueous solutions. The morphologies and the sizes of the two components were characterized by TEM, as shown in Fig. 2. It can be seen that the Au NCs were readily dispersed in water and possessed a good mono-dispersity with a particle size of about 2.0 nm (Fig. 2(a)). The diameter of C-dots was estimated to be 2.2 nm with a good dispersity (Fig. 2(b)). Additionally, the IR spectrum of C-dots (Fig. S4 in the ESM) shows a peak at 3,429 cm^{-1}, assigned to the O–H stretching vibration. Other vibrations at 2,985 and 1,402 cm^{-1} belong to the C–H stretching and deformation vibration. The characteristic vibration of C=O appears at 1,628 cm^{-1}, and the peak at 1,330 cm^{-1} is ascribed to the C–N stretch. These results indicate the existence of the carboxyl and the amide groups on the surface of the C-dots [26, 36, 37].

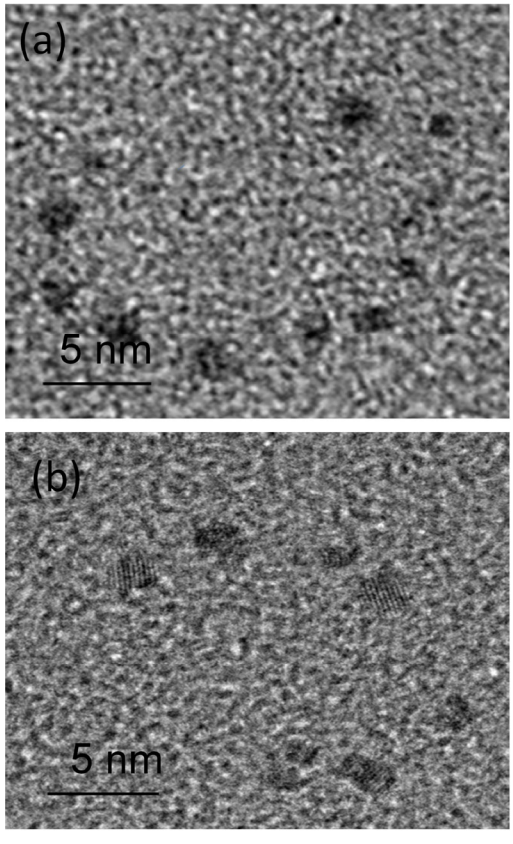

Figure 2 TEM images of the as-prepared (a) red emission of Au NCs and (b) blue emission of C-dots.

3.2 Characterization of the nanohybrid probe

The nanohybrid solution emits a strong pink fluorescence, as seen in Fig. 1(c), which is a different fluorescence color when compared to the Au NCs and

the C-dots. Also, the fluorescence spectrum of the dual-emission system displays two emission bands at 450 and 656 nm. As shown in Scheme 1, the fluorescence energy of C-dots lies in the blue range and is demonstrated to be stable against the mercury ion, which can serve as a better reference signal for Hg(II) assay. The Au NCs emits red fluorescence and is quenched by the mercury ion, which can serve as the reporter signal for Hg(II) detection. By combining the two fluorescence behaviors, an obvious fluorescence color change from pink to blue was achieved upon exposure to Hg(II), which can be applied for visual detection of the mercuric ions.

The analytical performance of the dual-emission nanohybrid deeply relied on the fluorescence intensities at 656 and 450 nm of I_{656}/I_{450}. The different intensity ratios of I_{656}/I_{450} were related to the amount of mercuric ions. When the I_{656}/I_{450} ratio for the nanohybrid was 3:1, the blue fluorescence was too weak to be observed in the presence of Hg(II), producing a narrow color change (Fig. S5 in the ESM). When the I_{656}/I_{450} intensity ratio was adjusted to 1:1, as shown in Fig. 3(a), a wider color variation from pink to blue was obtained. Other I_{656}/I_{450} intensity ratios such as, 2:1, did not result in an obvious color change (Fig. S6 in the ESM). Therefore, the I_{656}/I_{450} intensity ratio of 1:1 was selected as the optimal condition for the synthesis of the nanohybrid probe and the detection of mercuric ions. Additionally, the photostability of the nanohybrid probe was systematically studied and the results showed that the nanohybrid probe has good stability against photobleaching (Fig. S7 in the ESM).

3.3 Sensitivity of the nanohybrid probe for Hg(II)

Figure 3 represents the fluorescence detection of Hg(II) by the nanohybrid sensor. As can be seen in Fig. 3(a), the red emission at 656 nm from the Au NCs gradually decreased upon the addition of Hg(II). Unlike the role of the Au NCs in the nanohybrid sensor, the blue fluorescence at 450 nm from the C-dots was unchanged with the increase of Hg(II), resulting in self-calibration and a successive color change from pink to blue. On the other hand, the fluorescence intensity and color of the sole red Au NCs became weak when exposed to Hg(II), which was hard to be distinguished by the naked eye (Fig. 3(b)). The comparison clearly shows the advantages of the nanohybrid probe over the sole Au NCs, as a fluorescence probe.

Figure 4 shows that the fluorescence intensity ratio, I_{656}/I_{450} of the nanohybrid system decreased proportionately with increasing amounts of Hg(II), and a relationship can be set up between I_{656}/I_{450} and the Hg(II) concentration. A linear relation (range from 0 to 500 nM) with a coefficient R^2 of 0.997 was obtained

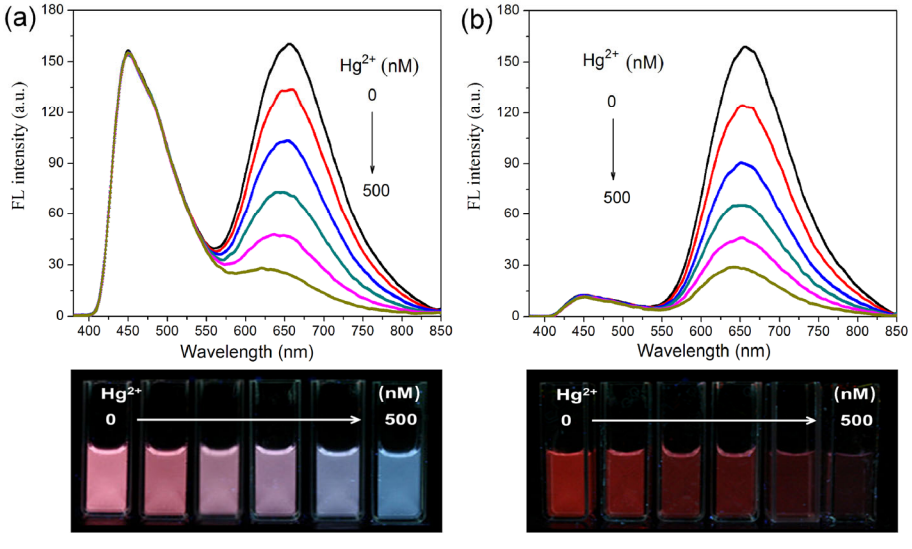

Figure 3 The fluorescence spectra of (a) the nanohybrid system and (b) the sole red Au NCs, in the presence of Hg(II) (0.0, 100, 200, 300, 400 and 500 nM). Inset: fluorescence images of the probe solution in the presence of various amounts of Hg(II) recorded under a 365 nm UV lamp.

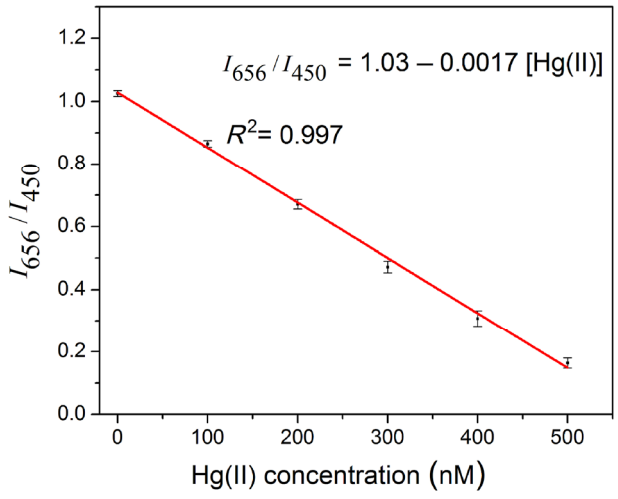

Figure 4 Fluorescence intensity ratio (I_{656}/I_{450}) of the nanohybrid system versus the concentration of Hg(II) (0.0, 100, 200, 300, 400 and 500 nM). The detection limit for Hg(II) was determined to be 28 nM based on the definition of 3 times deviation of the blank signal (3σ).

and the lowest amount of Hg(II) was determined to be 28 nM in aqueous solution. The decline of the fluorescence ratio (I_{656}/I_{450}) of the nanohybrid probe was attributed to the quenching of the red fluorescence of the Au NCs by Hg(II), which is consistent with the metallophilic Hg^{2+}–Au^{+} interactions [21, 30, 31]. The red fluorescence of the Au NCs could be partially recovered by the addition of sodium borohydride ($NaBH_4$, a strong reductant) to the Au NCs solution in the presence of Hg^{2+} ions [21]. This may be attributed to the reduction of Hg^{2+} to Hg^0 by $NaBH_4$. The latter has a weaker binding energy with Au^{+}, and thus a less quenching effect on the fluorescence (Fig. S8 in the ESM).

3.4 Selectivity of the nanohybrid probe study

To study the specificity of the sensing system for Hg(II) over other environmentally relevant metal ions, the fluorescence properties of the nanohybrid probe in the presence of various relevant metal ions (including Na(I), K(I), Ca(II), Mg(II), Ba(II), Zn(II), Co(II), Ni(II), Cd(II), Al(III), Fe(III), Pb(II), Cu(II)) were carefully examined, as shown in Fig. 5(a). There was little response in the presence of other metal ions at higher concentrations (1,000 nM), while Hg(II) (500 nM) dramatically quenched the red fluorescence. This result showed that the method has a good selectivity. In order to validate the method, anti-interference study of the nanohybrid probe for Hg(II) was further carried out (Fig. 5(b)) in the presence of the interfering metal ions. The intensity ratios, I_{656}/I_{450} of the nanohybrid probe do not change evidently after adding the metal ions (50 equiv. of Na(I), K(I), Ca(II), Mg(II), Ba(II), 10 equiv. of Zn(II), Co(II), Ni(II), Cd(II), Al(III), Fe(III), Pb(II), 2 equiv. of Cu(II)) to the probe solution. Later, 1 equiv. of Hg(II) (500 nM) was added to the mixture (Fig. S9 in the ESM). The results indicated that co-existence of these species have a negligible interfering effect on the Hg(II) sensing, suggesting the high selectivity of this method for Hg(II) over the other metal ions.

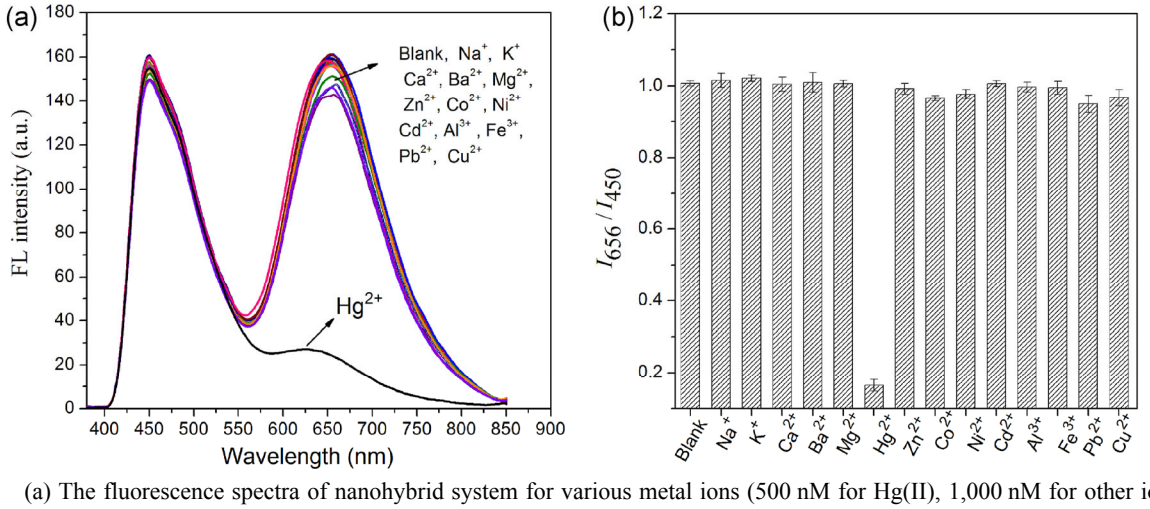

Figure 5 (a) The fluorescence spectra of nanohybrid system for various metal ions (500 nM for Hg(II), 1,000 nM for other ions). (b) The striped bars express the addition of 1 equiv. of Hg(II) (500 nM), other metal ions (50 equiv. of Na(I), K(I), Ca(II), Mg(II), Ba(II), 10 equiv. of Zn(II), Co(II), Ni(II), Cd(II), Al(III), Fe(III), Pb(II) and 2 equiv. of Cu(II)).

3.5 Detection of Hg(II) in real water samples

The present nanohybrid system was further validated for Hg(II) detection in real water samples including, lake water, tap water and mineral water. The lake water samples were obtained from Shushan Lake, a drinking water source. The water samples were first filtered through 0.45 μm Suporfilters to remove any suspended particles. The mineral water samples were bought from a local supermarket and the tap water samples were obtained from the city water supply. Both the mineral water and tap water samples were applied directly without any pretreatment. The original contents of Hg(II) in the samples of lake water, tap water, and mineral water were first determined to be 1.5, 1.1 and 0.2 nM, respectively by atomic absorbance spectrometry (TAS-990). These values were lower than the limits recommended by the World Health Organization (WHO) for drinking water (30 nM), so, they do not pose any health concerns. The spike and the recovery tests were then carried out with three different concentrations of Hg(II): 0, 230 and 460 nM in the three water samples and the results are presented in Table 1. As can be seen from Table 1, the recoveries in lake water samples are less than 100%, which could be caused by the humic substances, leading to a negative interference for the determination of the Hg(II). The recoveries in tap and mineral water samples are slightly more than 100%, which is consistent with the original contents of mercury. The results indicated that the method possesses the potential for practical applications such as on-site determination of mercury ion.

3.6 Paper-based sensor for visual detection of Hg^{2+}

For the purpose of on-site and rapid determination of mercuric ions, a fluorescence paper sensor was prepared. A series of 2.0 μL solutions containing the dual-emission solution was immobilized onto pieces of filter papers, 0.6 mm in diameter and then kept in the dark for 10 min to obtain uniform paper sensors. The as-prepared papers displayed orange-red fluorescence under UV lamp illumination. To visualize the mercury ions, 2.0 μL of different concentrations (0, 5, 10, 15, 20, and 30 μM) of the Hg(II) stocking solution was carefully dropped on the paper sensor to form a series of stained spots as shown in Fig. 6. Clearly, the colored spots from pink to blue were observed under a 365 nm UV lamp, which are dependent on the amount of Hg(II) added. Such a paper sensor could be used for on-site visual detection of Hg(II). This method showed comparable sensitivity and good selectivity with other methods used for mercury determination (Table S1 in the ESM).

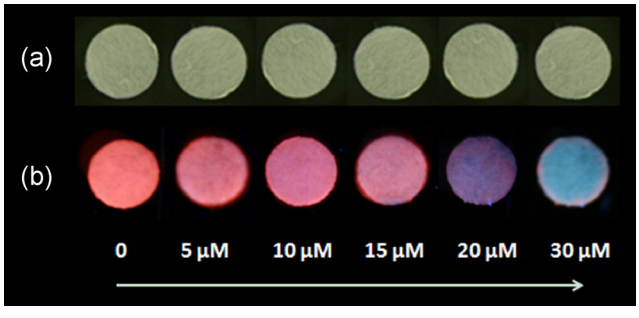

Figure 6 The images of the paper sensors after addition of various concentrations of Hg(II) solution (a) under daylight and (b) under a 365 nm UV lamp. The concentrations of Hg(II) from left to right were 0, 5, 10, 15, 20 and 30 μM.

4 Conclusions

In conclusion, we designed a ratiometrric fluorescence probe by hybridizing the C-dots and the Au NCs through surface bonding and other interactions. The nanohybrid probe exhibited dual emissions at 450 and

Table 1 Determination of mercury ion, Hg(II) using the nanohybrid probe in real water samples. The values are the average concentration of Hg(II) for each sample and were determined from three measurements

Add Hg (II) concentration (nM)	Lake water		Tap water		Mineral water	
	Found (nM)	Recovery (%)	Found (nM)	Recovery (%)	Found (nM)	Recovery (%)
0	5.6		15.9		11.7	
230	227	98.7 ± 2.1	246	107 ± 0.8	241	105 ± 1.7
460	434	94.3 ± 2.2	468	102 ± 0.5	462	101 ± 0.4

656 nm under a single excitation. The blue fluorescence at 450 nm was inert to Hg(II), while the red fluorescence showed good specificity to Hg(II), resulting in continuous fluorescence color changes from pink to blue with the increase of Hg^{2+} amount. The detection limit of this method was determined to be 28 nM in aqueous solution. Furthermore, we demonstrated that the nanohybrid could be used for preparation of paper sensors, which shows potential application for on-site and rapid determination of mercuric ions for pollution control.

Acknowledgements

This work was supported by National Natural Science Foundation of China (Nos. 21302187, 21475134, 21507135 and 91439101).

Electronic Supplementary Material: Supplementary material (the fluorescence spectra and images of nanohybrid probe before and after centrifugation and dialysis, the photostability of the Au NCs, C-dots and the nanohybrid probe, the FT-IR spectra of as-prepared C-dots, different intensity ratio I_{656}/I_{450} of the nanohybrid probe response to various concentration of Hg(II) and the comparison with other assays for mercury detection) is available in the online version of this article at http://dx.doi.org/10.1007/s12274-016-1099-5.

References

[1] Nolan, E. M.; Lippard, S. J. Tools and tactics for the optical detection of mercuric ion. *Chem. Rev*. **2008**, *108*, 3443–3480.

[2] Balaji, T.; El-Safty, S. A.; Matsunaga, H.; Hanaoka, T.; Mizukami, F. Optical sensors based on nanostructured cage materials for the detection of toxic metal ions. *Angew. Chem., Int. Ed*. **2006**, *45*, 7202–7208.

[3] Kozikowska, I.; Binkowski, Ł. J.; Szczepańska, K.; Sławska, H.; Miszczuk, K.; Śliwińska, M.; Łaciak, T.; Stawarz, R. Mercury concentrations in human placenta, umbilical cord, cord blood and amniotic fluid and their relations with body parameters of newborns. *Environ. Pollut*. **2013**, *182*, 256–262.

[4] Voegborlo, R. B.; Akagi, H. Determination of mercury in fish by cold vapour atomic absorption spectrometry using an automatic mercury analyzer. *Food Chem*. **2007**, *100*, 853–858.

[5] Tao, S. Q.; Gong, S. F.; Xu, L.; Fanguy, J. C. Mercury atomic absorption by mercury atoms in water observed with a liquid core waveguide as a long path absorption cell. *Analyst* **2004**, *129*, 342–346.

[6] O'Neil, G. D.; Newton, M. E.; Macpherson, J. V. Direct identification and analysis of heavy metals in solution (Hg, Cu, Pb, Zn, Ni) by use of *in situ* electrochemical X-ray fluorescence. *Anal. Chem*. **2015**, *87*, 4933–4940.

[7] Ohata, M.; Kidokoro, T. Effect of long-time X-ray irradiation on Cr and Hg in a polypropylene disk certified reference material observed during measurements by X-ray fluorescence spectrometry. *Anal. Sci*. **2015**, *31*, 855–858.

[8] Lv, J. T.; Luo, L.; Zhang, J.; Christie, P.; Zhang, S. Z. Adsorption of mercury on lignin: Combined surface complexation modeling and X-ray absorption spectroscopy studies. *Environ. Pollut*. **2012**, *162*, 255–261.

[9] Wan, C. C.; Chen, C. S.; Jiang, S. J. Determination of mercury compounds in water samples by liquid chromatography–inductively coupled plasma mass spectrometry with an *in situ* nebulizer/vapor generator. *J. Anal. At. Spectrom*. **1997**, *12*, 683–687.

[10] Li, B. H. Rapid speciation analysis of mercury by short column capillary electrophoresis on-line coupled with inductively coupled plasma mass spectrometry. *Anal. Methods* **2011**, *3*, 116–121.

[11] Lamble, K. J.; Hill, S. J. Determination of mercury in slurried samples by both batch and on-line microwave digestion-cold vapour atomic fluorescence spectrometry. *J. Anal. At. Spectrom.* **1996**, *11*, 1099–1103.

[12] Soomro, R. A.; Nafady, A.; Sirajuddin; Memon, N.; Sherazi, T. H.; Kalwar, N. H. L-cysteine protected copper nanoparticles as colorimetric sensor for mercuric ions. *Talanta* **2014**, *130*, 415–422.

[13] Liu, D. B.; Qu, W. S.; Chen, W. W.; Zhang, W.; Wang, Z.; Jiang, X. Y. Highly sensitive, colorimetric detection of mercury(II) in aqueous media by quaternary ammonium group-capped gold nanoparticles at room temperature. *Anal. Chem*. **2010**, *82*, 9606–9610.

[14] Kiatkumjorn, T.; Rattanarat, P.; Siangproh, W.; Chailapakul, O.; Praphairaksit, N. Glutathione and L-cysteine modified silver nanoplates-based colorimetric assay for a simple, fast, sensitive and selective determination of nickel. *Talanta* **2014**, *128*, 215–220.

[15] Zhu, Z. Q.; Su, Y. Y.; Li, J.; Li, D.; Zhang, J.; Song, S. P.; Zhao, Y.; Li, G. X.; Fan, C. H. Highly sensitive electrochemical sensor for mercury(II) ions by using a mercury-specific oligonucleotide probe and gold nanoparticle-based amplification. *Anal. Chem*. **2009**, *81*, 7660–7666.

[16] Tang, S. R.; Tong, P.; Lu, W.; Chen, J. F.; Yan, Z. M.; Zhang, L. A novel label-free electrochemical sensor for Hg^{2+} based on the catalytic formation of metal nanoparticle. *Biosens. Bioelectron.* **2014**, *59*, 1–5.

[17] Bhowmick, R.; Alam, R.; Mistri, T.; Bhattacharya, D.; Karmakar, P.; Ali, M. Morphology-directing synthesis of rhodamine-based fluorophore microstructures and application toward extra- and intracellular detection of Hg^{2+}. *ACS Appl. Mater. Interfaces* **2015**, *7*, 7476–7485.

[18] Yuan, Y.; Jiang, S. L.; Miao, Q. Q.; Zhang, J.; Wang, M. J.; An, L. N.; Cao, Q. W.; Guan, Y. F.; Zhang, Q.; Liang, G. L. Fluorescent switch for fast and selective detection of mercury (II) ions *in vitro* and in living cells and a simple device for its removal. *Talanta* **2014**, *125*, 204–209.

[19] Chen, T. H.; Lu, C. Y.; Tseng, W. L. One-pot synthesis of two-sized clusters for ratiometric sensing of Hg^{2+}. *Talanta* **2013**, *117*, 258–262.

[20] Lu, D. T.; Zhang, C. H.; Fan, L.; Wu, H. J.; Shuang, S. M.; Dong, C. A novel ratiometric fluorescence probe based on BSA assembled silver nanoclusters for mercuric ion selective sensing. *Anal. Methods* **2013**, *5*, 5522–5527.

[21] Xie, J. P.; Zheng, Y. G.; Ying, J. Y. Highly selective and ultrasensitive detection of Hg^{2+} based on fluorescence quenching of Au nanoclusters by Hg^{2+}–Au^{+} interactions. *Chem. Commun.* **2010**, *46*, 961–963.

[22] Bian, P. P.; Xing, L. W.; Liu, Z. M.; Ma, Z. F. Functionalized-tryptophan stabilized fluorescent Ag nanoclusters: Synthesis and its application as Hg^{2+} ions sensor. *Sens. Actuators B* **2014**, *203*, 252–257.

[23] Guo, C. L.; Irudayaraj, J. Fluorescent Ag clusters via a protein-directed approach as a Hg(II) ion sensor. *Anal. Chem.* **2011**, *83*, 2883–2889.

[24] Duan, J. L.; Song, L. X.; Zhan, J. H. One-pot synthesis of highly luminescent CdTe quantum dots by microwave irradiation reduction and their Hg^{2+}-sensitive properties. *Nano Res*. **2009**, *2*, 61–68.

[25] Xu, H.; Yang, X. P.; Li, G.; Zhao, C.; Liao, X. J. Green synthesis of fluorescent carbon dots for selective detection of tartrazine in food samples. *J. Agric. Food Chem*. **2015**, *63*, 6707–6714.

[26] Hsu, P. C.; Chang, H. T. Synthesis of high-quality carbon nanodots from hydrophilic compounds: Role of functional groups. *Chem. Commun*. **2012**, *48*, 3984–3986.

[27] Zhu, S. J.; Song, Y. B.; Zhao, X. H.; Shao, J. R.; Zhang, J. H.; Yang, B. The photoluminescence mechanism in carbon dots (graphene quantum dots, carbon nanodots, and polymer dots): Current state and future perspective. *Nano Res*. **2015**, *8*, 355–381.

[28] Xie, J. P.; Zheng, Y. G.; Ying, J. Y. Protein-directed synthesis of highly fluorescent gold nanoclusters. *J. Am. Chem. Soc.* **2009**, *131*, 888–889.

[29] Wen, F.; Dong, Y. H.; Feng, L.; Wang, S.; Zhang, S. C.; Zhang, X. R. Horseradish peroxidase functionalized fluorescent gold nanoclusters for hydrogen peroxide sensing. *Anal. Chem*. **2011**, *83*, 1193–1196.

[30] Chen, P. C.; Chiang, C. K.; Chang, H. T. Synthesis of fluorescent BSA-Au NCs for the detection of Hg^{2+} ions. *J. Nanopart. Res.* **2013**, *15*, 1336.

[31] Shang, L.; Yang, L. X.; Stockmar, F.; Popescu, R.; Trouillet, V.; Bruns, M.; Gerthsen, D.; Nienhaus, G. U. Microwave-assisted rapid synthesis of luminescent gold nanoclusters for sensing Hg^{2+} in living cells using fluorescence imaging. *Nanoscale* **2012**, *4*, 4155–4160.

[32] Zhang, X. L.; Xiao, Y.; Qian, X. H. A ratiometric fluorescent probe based on FRET for imaging Hg^{2+} ions in living cells. *Angew. Chem., Int. Ed*. **2008**, *47*, 8025–8029.

[33] Zhang, K.; Zhou, H. B.; Mei, Q. S.; Wang, S. H.; Guan, G. J.; Liu, R. Y.; Zhang, J.; Zhang, Z. P. Instant visual detection of trinitrotoluene particulates on various surfaces by ratiometric fluorescence of dual-emission quantum dots hybrid. *J. Am. Chem. Soc.* **2011**, *133*, 8424–8427.

[34] Yu, C. M.; Li, X. Z.; Zeng, F.; Zheng, F. Y.; Wu, S. Z. Carbon-dot-based ratiometric fluorescent sensor for detecting hydrogen sulfide in aqueous media and inside live cells. *Chem. Commun.* **2013**, *49*, 403–405.

[35] Cao, B. M.; Yuan, C.; Liu, B. H.; Jiang, C. L.; Guan, G. J.; Han, M. Y. Ratiometric fluorescence detection of mercuric ion based on the nanohybrid of fluorescence carbon dots and quantum dots. *Anal. Chim. Acta* **2013**, *786*, 146–152.

[36] Schroetter-Dirks, S.; Bougeard, D. Vibrational spectra of tris(hydroxymethyl)aminomethane hydrogenhalides $TRISH^{+}X^{-}$, $(HOH_2C)_3C–NH_3^{+}\cdot X^{-}$ (X = F, Cl, Br, I). *J. Mol. Struct*. **2003**, *661–662*, 109–119.

[37] Kumar, S.; Rai, A. K.; Singh, V. B.; Rai, S. B. Vibrational spectrum of glycine molecule. *Spectrochim. Acta A Mol. Biomol. Spectrosc*. **2005**, *61*, 2741–2746.